

# Synthesis and characterization of fluorescent polyphenols anchored Schiff bases via oxidative polycondensation

İSMET KAYA<sup>1,\*</sup>, FEYZA KOLCU<sup>1,2</sup>, SABRIYE SATILMIŞ<sup>1</sup>, ZEYNEP YAZICIOĞLU<sup>1</sup>

<sup>1</sup>Çanakkale Onsekiz Mart University, Department of Chemistry, Polymer Synthesis and Analysis Laboratory, 17020, Çanakkale, Turkey

<sup>2</sup>Çanakkale Onsekiz Mart University, Lapseki Vocational School, Department of Chemistry and Chemical Processing Technologies, Çanakkale, Turkey

A series of polyimines, bearing phenolic groups were successfully synthesized in aqueous alkaline solution via chemical oxidative polycondensation. Polymeric Schiff bases were synthesized by condensation of 2,4-dihydroxybenzaldehyde and 3-hydroxy-4-methoxybenzaldehyde with 2-aminophenol and 3-aminophenol. The molecular structures of the synthesized Schiff bases and their corresponding polymers were studied by FT-IR, UV-Vis, <sup>1</sup>H-NMR and <sup>13</sup>C-NMR spectroscopic methods. Thermal stability of the imine polymers was evidenced by their initial degradation temperatures found in the range of 170 °C to 271 °C without any sign of melting. The results of UV-Vis and cyclic voltammetry (CV) measurements were coherent with the optical  $E_g$  and the electrochemical  $E'_g$  band gaps of the polyimines which were lower than those of their corresponding Schiff bases. Fluorescence spectral analysis of P4 (Schiff base polymer P4 derived from 3-aminophenol and 3-hydroxy-4-methoxybenzaldehyde) revealed a bicolor emission with blue and green light. Electrical conductivity of the synthesized imine polymers was measured by four-point probe technique. P4 showed the highest electrical conductivity as a result of iodine vapor contact time. Morphology characterization of the synthesized polyimines was carried out using a scanning electron microscope SEM at different magnifications. The study revealed that P4 is a promising candidate for both blue and green light emitters which could be used in the production of photovoltaic materials and solar cells.

Keywords: Schiff base polycondensation; polyimines; polyphenols; blue-green light emitter; conductivity; SEM

## 1. Introduction

Recently, numerous research studies have been focused on polymers containing conjugated structures due to variety of their applications in many fields, such as electronics [1], optoelectronics [2], and photonics [3]. There is another class of conjugated polymer chain with imine (–CH=N–) moiety known as Schiff base polymer (or polyimine). Adams et al. [4] synthesized the first polyimine using condensation reaction between terephthaldehyde and benzidine or anisidine in 1923. In the late 1960s, polyimines have been used in aerospace applications and in the production of heat resistant materials and organic light emitting devices [5]. Since they included extended electronic states in the case of  $\pi$ -conjugated polymers, they have been also particularly widespread in the advanced

electronic devices with semiconducting properties such as battery devices, semiconductors, energy storage devices, and in electro-optics for switching and displays [6–8].

Polyphenols have been also popular owing to their easily oxidizable active hydroxyl groups which led to their widespread use in fields, such as semi-conductive, antistatic, antimicrobial materials, epoxy oligomers and block copolymers as adhesives, photoresists and antistatic materials [9, 10].

Oligophenols and their azomethine derivatives are synthesized using oxidative polycondensation (OP) reactions which are favored as they take place under moderate reaction conditions without toxic compounds. Attention has been paid to the polymer synthesis by OP due to using cheap and simple structured oxidants, easily separating the products from the reaction mixture, enhancing thermal

\*E-mail: kayaismet@hotmail.com

stability of the synthesized polymers, and releasing environmentally harmless by-products such as NaCl or KCl and H<sub>2</sub>O [11].

In the present study, to examine incorporation of different substituents into the polymers, we have focused on designing oxidative polycondensation of phenolic Schiff bases which carry hydroxyl and methoxy moieties. Schiff base polymers due to their semi-conductive properties are mainly used in the production of electrochemical cells and batteries and their conductivities can be increased by doping with iodine [12–14]. The effect of combining hydroxyl group and imine moieties along the polymer chain is mainly observed in the chemical oxidative polycondensation.

To reach this idea, the preliminary synthesis of Schiff base substituted polyphenols was performed and the obtained polymer was characterized by using FT-IR, UV-Vis, <sup>1</sup>H-NMR, <sup>13</sup>C-NMR, TG-DTA, SEC and PL techniques. The effect of hydroxyl group along the polymer chain on optical, electrical and thermal properties of the synthesized polymers was analyzed. This study presents the synthesis and characterization results of four polyimines bearing hydroxyl groups derived by condensation of 2,4-dihydroxybenzaldehyde and 3-hydroxy-4-methoxybenzaldehyde with 2-aminophenol and 3-aminophenol. The oxidative polycondensation (OP) resulted in obtaining a polymer blend with phenylene and oxyphenylene units as a result of carbon-carbon and carbon-oxygen couplings, respectively.

## 2. Experimental

### 2.1. Reagents

The starting materials to prepare Schiff base monomers: 2-aminophenol (2-AP, 99 %), 3-aminophenol (3-AP, 98 %), 2,4-dihydroxybenzaldehyde (2,4DHB, 98 %) and 3-hydroxy-4-methoxybenzaldehyde (3H4MB, 98 %) were supplied by Alfa Aesar, Across and Fluka, respectively. Ethanol, acetone, acetic acid, potassium hydroxide KOH, chloroform CHCl<sub>3</sub>, tetrahydrofurane THF, N,N'-dimethylformamide (DMF), (DMSO), toluene, acetonitrile, HCl (37 %)

and tetrabutylammonium hexafluorophosphate (TBAPF<sub>6</sub>) were supplied by Merck Chemical Co. (Germany). 30 % solution of sodium hypochloride was supplied by TEKKIM (Turkey). The reagents were used as received.

### 2.2. Preparation of the Schiff base monomers (S1, S2, S3 and S4)

Schiff base monomers S1 and S2 were synthesized using condensation reaction of 2-aminophenol (0.01 mol, 1.09 g) with 2,4-dihydroxybenzaldehyde (0.01 mol, 1.38 g) and 3-hydroxy-4-methoxybenzaldehyde (0.01 mol, 1.52 g), respectively [15]. In the same way, S3 and S4 were synthesized by a condensation reaction of 3-aminophenol (0.01 mol, 1.09 g) with 2,4-dihydroxybenzaldehyde (0.01 mol, 1.38 g) and 3-hydroxy-4-methoxybenzaldehyde (0.01 mol, 1.52 g), respectively. Schiff base monomers were synthesized by refluxing an ethanol solution of one of the aldehydes and one of the aminophenols in 1:1 ratio under constant stirring in a 250 mL three-necked round bottom flask fitted with a reflux condenser and magnetic stirrer at 80 °C for 5 h. The formed products were filtered, recrystallized from ethanol and dried in a vacuum oven at 40 °C for a day (yields: 82 %, 79 %, 85 % and 73 % for S1, S2, S3 and S4, respectively). The reaction procedure for the Schiff base monomers (S1, S2, S3 and S4) is shown in Fig. 1.

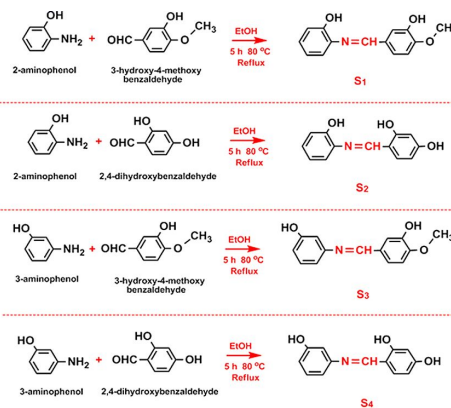


Fig. 1. Synthetic pathway of Schiff bases.

For S1: FT-IR (cm<sup>-1</sup>): 3320  $\nu$ (O–H), 3058  $\nu$  (C–H phenyl), 2932  $\nu$ (C–H aliphatic),

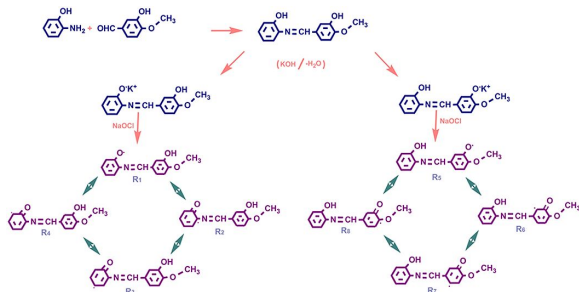


Fig. 2. Possible resonance species of S1.

1616  $\nu(\text{C}=\text{N})$ , 1437 to 1574  $\nu(\text{C}=\text{C}$  phenyl), 1250  $\nu(\text{C}-\text{OH})$ .  $^1\text{H}$  NMR (DMSO- $d_6$ ):  $\delta$ , ppm, 9.42 (s, 1H,  $-\text{OH}$ ), 9.27 (s, 1H,  $-\text{OH}$ ), 8.33 (s, 1H,  $-\text{HC}=\text{N}$ ) 7.36 (d, 1H,  $\text{H}_d$ ), 7.24 (t, 1H,  $\text{H}_b$ ), 7.12 (t, 1H,  $\text{H}_c$ ), 6.99 (d, 1H,  $\text{H}_g$ ), 6.58 (d, 1H,  $\text{H}_f$ ), 6.53 (d, 1H,  $\text{H}_a$ ), 5.96 (s, 1H,  $\text{H}_e$ ), 3.79 (s, 3H,  $-\text{OCH}_3$ ).  $^{13}\text{C}$  NMR (DMSO- $d_6$ ):  $\delta$ , ppm, 160.18 (C7), 158.58 (C1-*ipso*), 153.68 (C10-*ipso*), 151.30 (C11-*ipso*), 150.44 (C6-*ipso*), 147.30 (C4-*ipso*), 130.32 (C3), 129.65 (C8-*ipso*), 122.72 (C13), 114 (C5), 113 (C2), 112.10 (C9), 108.30 (C12), 56.14 ( $-\text{OCH}_3$ ).

For S2: FT-IR ( $\text{cm}^{-1}$ ): 3100  $\nu(\text{O}-\text{H})$ , 2900  $\nu(\text{C}-\text{H}$  phenyl), 1614  $\nu(\text{C}=\text{N})$ , 1585  $\nu(\text{C}=\text{C}$  phenyl), 1222  $\nu(\text{C}-\text{OH})$ .  $^1\text{H}$  NMR (DMSO- $d_6$ ):  $\delta$ , ppm, 10.20 (s, 1H,  $-\text{OH}$ ), 9.54 (s, 2H,  $-\text{OH}$ ), 8.69 (s, 1H,  $-\text{HC}=\text{N}$ ) 7.37 (d, 1H,  $\text{H}_d$ ), 7.16 (t, 1H,  $\text{H}_b$ ), 6.71 (d, 1H,  $\text{H}_f$ ), 6.66 (t, 1H,  $\text{H}_c$ ), 6.62 (d, 1H,  $\text{H}_g$ ), 6.36 (d, 1H,  $\text{H}_a$ ), 6.25 (s, 1H,  $\text{H}_e$ ).  $^{13}\text{C}$  NMR (DMSO- $d_6$ ):  $\delta$ , ppm, 163.74 (C7), 163 (C9-*ipso*), 162.79 (C11-*ipso*), 158.82 (C1-*ipso*), 149.78 (C6-*ipso*), 134.97 (C13), 130.64 (C3), 113.91 (C8-*ipso*), 112.50 (C4), 112.25 (C5), 108.38 (C2, C12), 102.92 (C10).

For S3: FT-IR ( $\text{cm}^{-1}$ ): 3219  $\nu(\text{O}-\text{H})$ , 2952  $\nu(\text{C}-\text{H}$  phenyl), 2839  $\nu(\text{C}-\text{H}$  aliphatic), 1610  $\nu(\text{C}=\text{N})$ , 1503  $\nu(\text{C}=\text{C}$  phenyl), 1271  $\nu(\text{C}-\text{OH})$ .  $^1\text{H}$  NMR (DMSO- $d_6$ ):  $\delta$ , ppm, 9.26 (s, 1H,  $-\text{OH}$ ), 8.75 (s, 1H,  $-\text{OH}$ ), 8.31 (s, 1H,  $-\text{HC}=\text{N}$ ) 7.35 (s, 1H,  $\text{H}_d$ ), 7.22 (d, 1H,  $\text{H}_a$ ), 7.09 (t, 1H,  $\text{H}_b$ ), 6.98 (d, 1H,  $\text{H}_g$ ), 6.70 (d,  $\text{H}_f$ ), 6.57 (d, 1H,  $\text{H}_c$ ), 5.94 (s, 1H,  $\text{H}_e$ ), 3.77 (s, 3H,  $-\text{OCH}_3$ ).  $^{13}\text{C}$  NMR (DMSO- $d_6$ ):  $\delta$  ppm, 160.19 (C7), 158.58 (C4-*ipso*), 153.68 (C10-*ipso*), 151.37 (C11-*ipso*),

150.5 (C6-*ipso*), 147.30 (C1), 130.34 (C2), 129.74 (C8-*ipso*), 122.89 (C13), 114.06 (C3), 113.08 (C5), 112.12 (C9), 108.31 (C12), 56.14 ( $-\text{OCH}_3$ ).

For S4: FT-IR ( $\text{cm}^{-1}$ ): 3047  $\nu(\text{O}-\text{H})$ , 2968  $\nu(\text{C}-\text{H}$  phenyl), 1623  $\nu(\text{C}=\text{N})$ , 1590  $\nu(\text{C}=\text{C}$  phenyl).  $^1\text{H}$  NMR (DMSO- $d_6$ ):  $\delta$ , ppm, 10.20 (s, 1H,  $-\text{OH}$ ), 9.54 (s, 2H,  $-\text{OH}$ ), 8.71 (s, 1H,  $-\text{HC}=\text{N}$ ) 7.37 (d, 1H,  $\text{H}_a$ ), 7.16 (t, 1H,  $\text{H}_b$ ), 6.73 (d, 1H,  $\text{H}_f$ ), 6.67 (s, 1H,  $\text{H}_d$ ), 6.64 (d, 1H,  $\text{H}_g$ ), 6.36 (d, 1H,  $\text{H}_c$ ), 6.25 (s, 1H,  $\text{H}_e$ ).  $^{13}\text{C}$  NMR (DMSO- $d_6$ ):  $\delta$ , ppm, 163.77 (C7), 163 (C4-*ipso*), 162.77 (C9-*ipso*), 158.82 (C11-*ipso*), 149.55 (C6-*ipso*), 134.97 (C1), 130.64 (C2), 113.91 (C8-*ipso*), 112.50 (C13), 112.25 (C3), 108.38 (C5), 108.36 (C12), 102.92 (C10).

### 2.3. Preparation of the Schiff base polymers (P1, P2, P3 and P4)

S1, S2, S3 and S4 were used to synthesize the corresponding polymers (P1, P2, P3 and P4).

1.50 g of the preliminary synthesized Schiff base was dissolved in a two necked round bottom flask with an attached reflux condenser and magnetic stirrer containing potassium hydroxide (10 % in water). 1 mL of NaOCl (30 % in water) was added into the flask within 20 min. The temperature of the reaction mixture was maintained at 90 °C for 25 h. Then, the reaction mixture was neutralized upon mixing 0.025 mol HCl (37 %) solution when it was cooled to room temperature. The resulting polymers quickly precipitated from the reaction solution as a result of a fast proceeding reaction. The polymerization pathway and the radical species are outlined in Fig. 2 and Fig. 3. The polymeric precipitates were filtered, washed several times with water to remove the mineral salts and dried in a vacuum oven [16]. The yields of P1, P2, P3 and P4 were found to be 81 %, 63 %, 69 % and 64 %, respectively.

For P1: FT-IR ( $\text{cm}^{-1}$ ): 3353  $\nu(\text{O}-\text{H})$ , 3197  $\nu(\text{C}-\text{H}$ , phenyl), 2805  $\nu(\text{C}-\text{H}$ , aliphatic), 1640  $\nu(\text{C}=\text{N})$ , 1457 to 1578  $\nu(\text{C}=\text{C}$ , phenyl), 1250  $\nu(\text{C}-\text{OH})$ .  $^1\text{H}$  NMR (DMSO- $d_6$ ):  $\delta_{\text{H}}$  ppm, 10.20 (s,  $-\text{OH}$ ), 9.58 (s,  $-\text{OH}$ ), 9.90 (s,  $-\text{OH}$ ), 8.44 (s, 1H,  $-\text{HC}=\text{N}$ ), 7.36 (s,  $\text{H}_d$ ), 7.22 (s,  $\text{H}_b$ ), 7.08 (s,  $\text{H}_g$ ), 6.27 (s,  $\text{H}_e$ ), 3.82 (s,  $-\text{OCH}_3$ ).  $^{13}\text{C}$  NMR

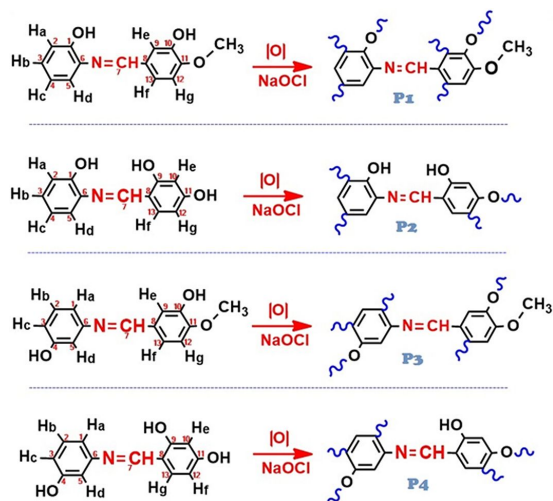


Fig. 3. Syntheses of polymers.

(DMSO- $d_6$ ):  $\delta$  ppm, 160.45 (C7), 159.74 (C1), 153.89 (C10), 151.23 (C6), 147.58 (C4), 147.06 (C6), 130.35 (C3), 124.93 (C8), 122.79 (C13), 119.94 (C5), 116.32 (C2), 114.02 (C9), 112.12 (C12), 56.32 ( $-OCH_3$ ).

For P2: FT-IR ( $cm^{-1}$ ): 3328  $\nu(O-H)$ , 2988  $\nu(C-H)$  phenyl, 1638  $\nu(C=N)$ , 1507  $\nu(C=C)$  phenyl, 1229  $\nu(C-OH)$ .  $^1H$  NMR (DMSO- $d_6$ ):  $\delta$ , ppm, 10.20 (s,  $-OH$ ), 8.79 (s,  $-HC=N$ ) 7.50 to 6.27 (m, aromatic).  $^{13}C$  NMR (DMSO- $d_6$ ):  $\delta$ , ppm, 161.61 (C7), 159.26 (C9-*ipso*), 150.74 (C11-*ipso*), 149.74 (C1-*ipso*), 147.02 (C6-*ipso*), 142.63 (C13), 134.24 (C3), 127.20 (C8-*ipso*), 125.44 (C4), 123.75 (C5), 119.99 (C2), 116.54 (C12), 103.90 (C10).

For P3: FT-IR ( $cm^{-1}$ ): 3200  $\nu(O-H)$ , 3020  $\nu(C-H)$  phenyl, 2837  $\nu(C-H)$  aliphatic, 1618  $\nu(C=N)$ , 1578  $\nu(C=C)$  phenyl, 1276  $\nu(C-OH)$ .  $^1H$  NMR (DMSO- $d_6$ ):  $\delta$ , ppm, 9.25 (br, OH), 8.58 (br,  $-OH$ ), 8.43 (s,  $-HC=N$ ), 7.35-6.0 (m, aromatic hydrogens), 7.35 (d,  $H_d$ ), 7.21 (s,  $H_b$ ), 7.06 (s,  $H_g$ ), 3.82 (s,  $-OCH_3$ ).  $^{13}C$  NMR (DMSO- $d_6$ ):  $\delta$ , ppm, 159.27 (C7), 158.84 (C4-*ipso*), 153.91 (C10-*ipso*), 151 (C11-*ipso*), 150.5 (C6-*ipso*), 145.98 (C1-*ipso*), 130.33 (C2), 130.01 (C8-*ipso*), 124.96 (C13), 117.18 (C9), 114.01 (C3-*ipso*), 113 (C5), 112.12 (C9), 108.32 (C12), 102.46 (C13), 56.13 ( $-OCH_3$ ).

For P4: FT-IR ( $cm^{-1}$ ): 3233  $\nu(O-H)$ , 3063  $\nu(C-H)$  phenyl, 1640  $\nu(C=N)$ , 1590  $\nu(C=C)$  phenyl.

## 2.4. Instrumentation

1 mg of sample and 1 mL of solvent were combined to carry out the solubility test in various solvents at room temperature. Fourier transform infrared (FT-IR) spectrometry (PerkinElmer FT-IR) with ATR sampling accessory in the wave number range of  $650\text{ cm}^{-1}$  to  $4000\text{ cm}^{-1}$ , (USA) was employed to identify the functional groups in the polymers. Polymer samples were dissolved in dimethyl sulfoxide- $d_6$  to obtain  $^1H$  and  $^{13}C$ -NMR spectra using JNM-ECX series (Japan) performed in the range of 400 MHz and 100.6 MHz, respectively. As the internal reference, tetramethylsilane was used in NMR measurements, SEC analyses enabled to find the number-average molecular weight  $M_n$ , the average molecular weight  $M_w$  and polydispersity index PDI. To calibrate the instrument (Shimadzu 10AVp series HPLC-SEC system), polystyrene standards (Polymer Laboratories), the peak molecular weights,  $M_p$ , between 162 and 60,000, SGX (100 Å and 7.7 nm diameter) and DMF as eluent were used in the analyses at a flow rate of  $0.4\text{ mL}\cdot\text{min}^{-1}$ .

Ultraviolet-visible (UV-Vis) spectra were performed at  $25\text{ }^\circ\text{C}$  in DMSO using Analytik Jena Specord 210 Plus (United Kingdom). To obtain photoluminescence properties of the samples in DMSO, a Shimadzu RF-5301PC spectrofluorophotometer (Japan) was employed. Slit width in PL measurements was specified as 5 nm.

Thermogravimetric and differential thermal analyses (TG-DTG-DTA) using PerkinElmer Pyris Sapphire (USA) were implemented to determine the mass change regarding to thermal degradation of the polymers under nitrogen flow of  $200\text{ mL}\cdot\text{min}^{-1}$  from ambient temperature up to  $1000\text{ }^\circ\text{C}$  at a heating rate of  $10\text{ }^\circ\text{C}\cdot\text{min}^{-1}$ . Differential scanning calorimetry (DSC, PerkinElmer Sapphire) was used to determine the glass transition temperature  $T_g$  of the synthesized polymer

samples in the temperature range of 25 °C to 420 °C under nitrogen atmosphere at a heating rate of 10 °C·min<sup>-1</sup>.

Conductivity measurements of the polymers were carried out by four-point probe technique using Keithley 2400 Electrometer at room temperature and atmospheric pressure. The polymers were pressed into pellets at a pressure of 1687.2 kg·cm<sup>-2</sup>. The pellet samples were doped with iodine vapor in a desiccator at room temperature. Electrical conductivities of the iodine doped polymers with respect to time were recorded.

Particles morphology was investigated using JEOL JSM 7100F field emission scanning electron microscopy (FE-SEM). Sputter coating process was used to create a thin gold/palladium film on the polymer samples.

Electrochemical experiments were performed on a CHI 660C Electrochemical Analyzer (CH Instrument, Texas, USA) equipped with three-electrode cell consisting of a carbon working microelectrode, a platinum auxiliary electrode and a non-aqueous Ag/Ag<sup>+</sup> reference electrode. All electrochemical potentials of cyclic voltammetry CV measurements were reported with respect to the external ferrocene-ferrocenium Fc/Fc<sup>+</sup> couple standard. All experiments were carried out at room temperature, in a dry box filled with argon. The half-wave potentials E<sup>1/2</sup> of Fc/Fc<sup>+</sup> in 0.1 M acetonitrile solution of TBAPF<sub>6</sub> were measured as 0.39 V and 0.38 V with respect to Ag wire and supporting calomel electrolyte, respectively. Cyclic voltammetric analyses were carried out in acetonitrile for the synthesized Schiff bases and polymers P1, P2, P3 and acetonitrile/DMSO mixture (v/v: 4/1) for P4. The electrochemical HOMO and LUMO energy levels and band gaps E'<sub>g</sub> of the polymers were calculated using oxidation and reduction onset values of the compounds.

### 3. Results and discussion

#### 3.1. Characterization of the synthesized Schiff bases and their imine polymers

P1, P2 and P3 are soluble in polar aprotic solvents, such as DMSO and DMF despite

of partial solubility in some polar solvents, such as acetonitrile and ethanol. P4 is insoluble in polar protic solvents while partially soluble in polar aprotic solvents such as DMSO and acetonitrile. On the other hand, all synthesized polymers are insoluble in non-polar solvents such as n-hexane and toluene. The color of S1 and S3 was brown; S2 and S4 was yellow, in comparison with their corresponding polymers which were black colored.

In the oxidative polymerization of phenolic compounds, the formation of a phenoxy radical, followed by the dimerization of other radical kinds via radical coupling, takes place [17]. Possible resonance structures during the progress of polymerization of S1 are given in Fig. 2 to compare eight main coupling sites in an aqueous alkaline medium by the oxidative polycondensation method. Since -OH group is ortho and para directing group in the aromatic ring, the polymer formation is expected to proceed from carbon radicals positioned at C2, C4, C10 and C13. According to Fig. 3, the radical at the oxidized state could be extended through the Schiff base and hereby, the polymerization could progress at both sides of the Schiff bases.

FT-IR spectra values of the synthesized Schiff bases and their imine polymers are given in the experimental procedure section. The structures of the synthesized compounds were confirmed by the presence of characteristic absorption peaks in the respective regions. FT-IR spectra of S1, S2, S3 and S4 and P1, P2, P3 and P4 elucidated that the stretching vibrations of imine bond (C=N) observed in the range of 1600 cm<sup>-1</sup> to 1618 cm<sup>-1</sup> proved the molecular structures of Schiff bases. The characteristic peaks of O-H stretching modes of all synthesized compounds were observed in the range of 3047 cm<sup>-1</sup> to 3360 cm<sup>-1</sup>. They transformed into broader peaks for the polymers due to extended conjugation along the chain as a result of polymerization of Schiff bases. The absorption peaks in the range of 2839 cm<sup>-1</sup> to 3060 cm<sup>-1</sup> attributed to the stretching modes of aromatic C-H bonds existing in S1, S2, S3 and S4 were observed in the range of 2988 cm<sup>-1</sup> to 3063 cm<sup>-1</sup> in P1, P2, P3 and P4. The peaks of aliphatic C-H stretching modes caused by the presence

of methoxy ( $-\text{OCH}_3$ ) group, observed at  $2932\text{ cm}^{-1}$  and  $2839\text{ cm}^{-1}$  for S1 and S3, shifted to  $2805\text{ cm}^{-1}$  and  $2837\text{ cm}^{-1}$  for P1 and P3, respectively. Broadening of the peaks belonging to the aromatic region in the polymer spectrum was the evidence of an effective oxidative polymerization [18].

Spectral peaks that could provide structural confirmation for Schiff bases S2 and S4 derived from 2,4-dihydroxybenzaldehyde, showed that relatively intense peaks assignable to  $\nu(\text{C}=\text{N})$  were detected at  $1614\text{ cm}^{-1}$  to  $1623\text{ cm}^{-1}$  for the synthesized Schiff bases possessing the formula of  $\text{Ar}-\text{CH}=\text{N}-\text{Ar}$ . The presence of intermolecular hydrogen bonds between the hydroxyl oxygen and the nitrogen atom could be detected around  $1700\text{ cm}^{-1}$  for  $\text{C}=\text{O}$  group of the keto-amine tautomer or the unreacted aldehyde. However, S2 and S4 did not show an absorption band at about  $1700\text{ cm}^{-1}$  since they were in phenol-imine structure.

$^1\text{H}$  NMR spectra of S1, S2, S3 and S4 were placed on record to compare to those of polymers. The  $^1\text{H}$  and  $^{13}\text{C}$ -NMR peak values of other synthesized compounds were given in the experimental procedure part. A characteristic feature of the conjugated polymers was the shift of the hydrogen signals to lower fields after polymerization. Fig. 3 elucidates that the synthetic route of P1 proceeded from the radicals ortho and para positioned to  $-\text{OH}$  (R3, R4, R6 and R7), and phenoxide radicals at both of the  $-\text{OH}$  protons (R1 and R5) via the formation of  $\text{C}-\text{C}$  and  $\text{C}-\text{O}-\text{C}$  couplings, respectively. The proton signals at 5.96 ( $\text{H}_a$ ), 7.16 ( $\text{H}_c$ ), 9.27 ( $\text{OH}$ ) and 9.47 ppm ( $\text{OH}$ ) for S1 almost disappeared as a result of polymerization. But at the spectrum of P1, the singlet peak was particularly observed at 6.27 ppm for He which was positioned at 5.96 ppm as a singlet in the  $^1\text{H}$  NMR of S1. The reason was likely that the polymerization through  $\text{C}-\text{C}$  coupling at C9 (R6) was not allowed since the steric hindrance emerged as a result of the polymerization through  $\text{C}-\text{O}-\text{C}$  coupling at C1 radical (R1). The decrease in the intensities of the signals indicates that the oxidative polymerization took place over the radicals formed at C1, C2, C4, C10 and C13. The electronegativity of oxygen

atom in hydroxyl group caused the proton signal of  $\text{OH}$  to move downfield in the  $^{13}\text{C}$  NMR spectra. The intensities of C2 and C4 peaks decreased since the polymerization path was through the radicals forming ortho and para positions to  $\text{OH}$  (R4 and R3, respectively). A linkage between two benzene units formed via  $\text{C}-\text{C}$  coupling led to the shifts of the ortho and para carbon signals downfield. These findings clarified that polymerization of S1 primarily took place through C2, C4 and C13 phenylene and C1 and C10 oxyphenylene units.

$^1\text{H}$  NMR signals of  $-\text{OH}$  and  $-\text{CH}=\text{N}-$  groups for S2 were observed at 10.20 ppm, 9.54 ppm and 8.69 ppm, respectively. According to the spectrum of P2, the signal at 9.54 ppm for the hydroxyl protons of S2 disappeared, proving that the oxidative polymerization primarily took place via  $\text{C}-\text{O}-\text{C}$  couplings at C9 and C11 (Fig. 4 and Fig. 5). The other possibility for the formation of phenoxide radical on C1 (R1) could be disproved by uniform intensity of C1 signal for S1 and P1. There was no particular decrease in the signal of  $\text{OH}$  proton on C1. The proton signals observed at 6.25 ( $\text{H}_e$ ) and 6.36 ppm ( $\text{H}_a$ ) for S2 ceased to be visible after the polymerization. Broadening in the peaks for aromatic hydrogens was an indication of polymerization process.

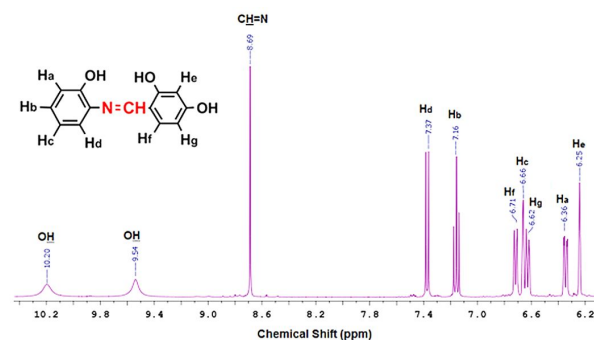
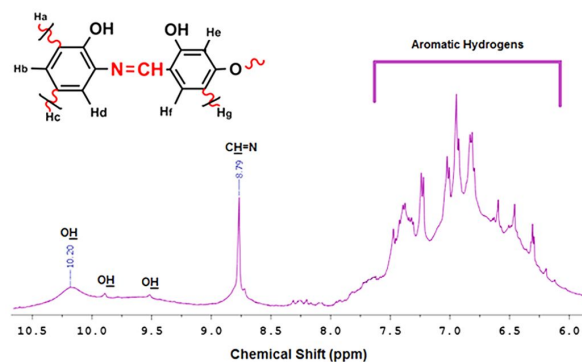
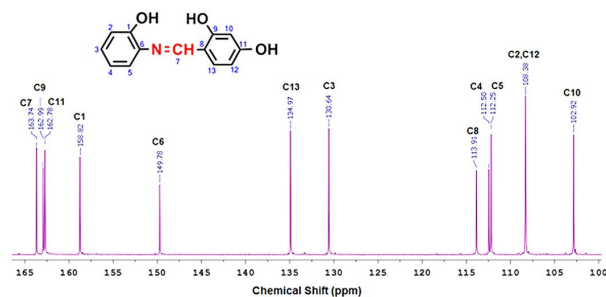
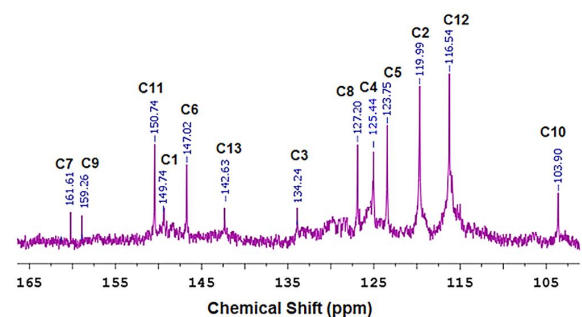


Fig. 4.  $^1\text{H}$  NMR spectrum of S2.

Evidently, the coexistence of both carbon signals for azomethine at 163.74 ppm and hydroxyl functions at 163.0 ppm, 162.79 ppm and 158.82 ppm in the  $^{13}\text{C}$  NMR spectra of S2 could be ascribed to the creation of phenol-imine structure (Fig. 6 and Fig. 7). The intensities of C2, C4,

Table 1. SEC analyses results of the synthesized polymers.

Compounds	Total			Fraction I				Fraction II			
	M <sub>n</sub>	M <sub>w</sub>	PDI	M <sub>n</sub>	M <sub>w</sub>	PDI	%	M <sub>n</sub>	M <sub>w</sub>	PDI	%
P1	9100	13300	1.46	30000	66000	2.20	15	16200	19700	1.21	85
P2	12700	14900	1.17	72500	85400	1.17	25	9800	11300	1.15	75
P3	12050	13850	1.15	33250	45400	1.37	60	10400	11800	1.13	40
P4	12500	15200	1.22	43700	54600	1.24	40	12500	14300	1.14	60

Fig. 5. <sup>1</sup>H NMR spectrum of P2.Fig. 6. <sup>13</sup>C NMR spectrum of S2.Fig. 7. <sup>13</sup>C NMR spectrum of P2.

C10 and C12 decreased after polymerization, substantiating that the polymerization of S2 primarily took place via C2, C4, C10, C12 phenylene and C9, C11 oxyphenylene units.

The broadening of signals for the aromatic protons observed in the range of 6.0 ppm to 7.50 ppm notified the presence of repeating aromatic units with several chemical surroundings. Due to the appearance of imine (–CH=N–) bond, the incoming signals related to the imine bond were observed at 8.31 ppm and 8.69 ppm for S3 and S4, respectively. Since the signals for both of the OH protons were not observed in the <sup>1</sup>H NMR spectra of P3, the oxidative polymerization proceeded by C–O–C coupling path. The proton signals at 5.94 (He), 6.57 (Hc) and 7.22 ppm (Ha) for S3 disappeared as a result of polymer formation. Finally, P3 was formed through the radicals ortho and para positioned to hydroxyl groups, and the polymerization took place via C–C coupling. Additionally, according to <sup>13</sup>C NMR spectra, the peaks were deshielded as a consequence of coupling carbon radicals compared to those of Schiff bases owing to an increase in the conjugation length. In comparison of S3 to P3, the peak value of C3 shifted from 114.06 ppm to 117.18 ppm. The other significant observation was that the signal observed at 7.35 ppm for Hd was still seen as a singlet at 7.35 ppm in the <sup>1</sup>H NMR spectrum of P3. The proposed structures of the polymers were evidenced by virtue of the NMR analyses concurrent with the UV-Vis and FT-IR analyses. The estimated polymerization route of S4 could be that phenoxide radicals (C4, C9 and C11) were formed through the oxidation of OH protons, concluded by polymerization via C–O–C coupling. There were three other possible radicals ortho and

para positioned to hydroxyl groups, which resulted in the polymerization through C–C coupling. The findings clarified that polymerization of S4 mainly took place via C1, C3, C10 and C12 phenylene and C4, C9 and C10 oxyphenylene units. Since P4 was partially soluble in DMSO, the polymerization took place through all possible radicals.

The number-average molecular weight  $M_n$ , the weight-average molecular weight  $M_w$  and the polydispersity index PDI values were tabulated in Table 1 depending on the results of SEC chromatograms. The average molecular weights of the polymers were found to be in the range of 13300 Da to 15200 Da with PDI of 1.15 to 1.46, suggesting a narrow distribution of molecular weight. Polyimines P2 and P4 had the highest molecular weight since  $^1\text{H}$  NMR analyses confirmed the structures of P2 and P4 with highly probable radicals for the polymerization; as a result, P2 and P4 were highly polymeric structured. According to the average molecular weight, P1, P2, P3 and P4 had nearly 40 to 56, 56 to 66, 50 to 58 and 55 to 67 repeated units, respectively.

### 3.2. Thermal properties of the synthesized polymers

To gain more comprehension about the properties of imine polymers, thermal degradation analyses of the synthesized compounds were carried out by TG analysis under inert nitrogen atmosphere with a heating rate of  $10\text{ }^\circ\text{C}\cdot\text{min}^{-1}$ . The TG curves for the synthesized Schiff bases and their corresponding polyimines are shown in Fig. 8. Thermal analyses results (TG, DTG, DTA and DSC) regarding to the synthesized compounds were summarized in Table 2. As seen in Table 2, TG-DTG analyses explicated that P1 and P4 degraded in three steps, while P2 and P3 in two steps. As seen in Fig. 8, 3.40 % and 4.0 %; 10.20 % and 10.70 % weight losses assigned to the elimination of volatile components, such as adsorbed water and solvent for P1 and P2, P3 and P4 were observed around 60 °C to 120 °C and 60 °C to 150 °C, respectively [19]. The initial degradation temperatures  $T_{\text{on}}$  of the polymers, P1, P2, P3 and P4 were calculated as 170 °C, 219 °C, 271 °C and 188 °C, respectively.

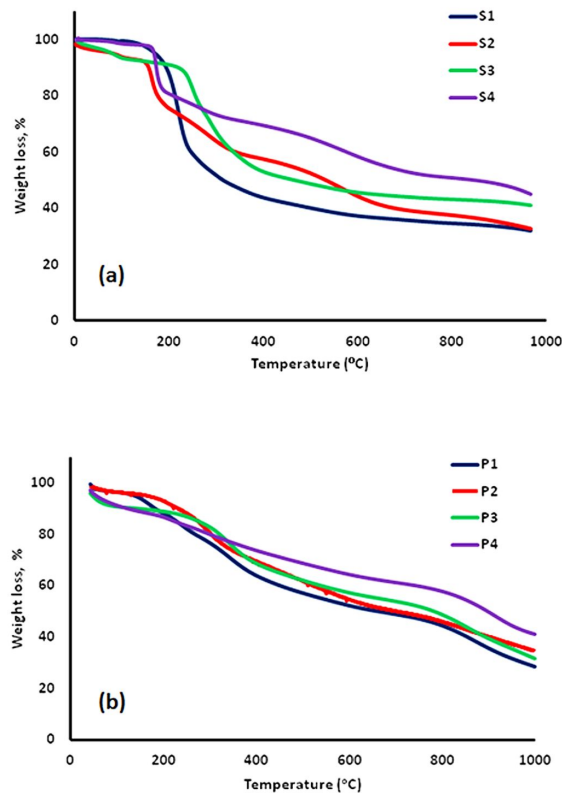


Fig. 8. TG profiles of the synthesized Schiff bases (a), and their imine polymers (b).

The polymers started to decompose at 170 °C to 271 °C without any sign of melting. The observed weight loss was 47.04 %, 46.11 %, 34.65 % and 27.63 % for P1, P2, P3 and P4, respectively, at the first degradation, where the highest weight loss of 20 % of the initial weights for P1, P2, P3 and P4 took place at 305 °C, 327 °C, 386 °C and 481 °C. The temperatures corresponding to 50 % weight loss were observed at 771 °C, 792 °C and 899 °C for P1, P2 and P3, respectively. The polyaromatic units formed by C–O–C couplings were firstly degraded, then, degradation of the C–C couplings occurred. Additionally, the char % amounts of the polymers at 1000 °C were listed in Table 2, informing that the maximum value of 52.45 % was obtained for P4 with thermostable properties due to the fact that its long conjugation increased the delocalization of  $\pi$ -electrons.

Differential scanning calorimeter DSC technique was another approach to determine

thermal properties of the polymers. Based on the DSC curves of the polymers, the glass transition temperatures  $T_g$  were found to be 109 °C, 130 °C, 139 °C and 134 °C for P1, P2, P3 and P4, respectively.

### 3.3. Optical and electrochemical properties

The optical absorption spectra of S1, S2, S3 and S4 and their corresponding polyimines are shown in Fig. 9. All the polyimines show two clear absorption peaks in the measured absorption spectrum. The peaks of  $\pi \rightarrow \pi^*$  electronic transition for the aromatic ring in the polymer chain and characteristic absorption of  $n \rightarrow \pi^*$  transitions for azomethine ( $-\text{CH}=\text{N}$ ) group of the synthesized Schiff bases are observed in the ranges of 280 nm to 300 nm and 360 nm to 370 nm, respectively. Bilge *et al.* [20] explained that the keto-imine form of Schiff bases using salicylaldehyde was not observed in polar and non-polar solvents. No absorption bands were detected above 400 nm in DMSO for  $n \rightarrow \pi^*$  transition of  $\text{C}=\text{O}$  group. Similarly, there was no band observed above 400 nm indicating the presence of  $\text{C}=\text{O}$  functions in the structure of S2 and S4 derived from 2,4-dihydroxybenzaldehyde. Peaks related to  $\pi \rightarrow \pi^*$  electronic transitions were red shifted due to polymerization, which was common for conductive polymers. The optical band gap values  $E_g$  were obtained using  $E_g = 1242/\lambda_{\text{onset}}$  [21], where  $\lambda_{\text{onset}}$  is the starting wavelength for the electronic transition (the onset wavelength) identified by intersection of two tangents on the absorption edges. Table 3 elucidates that the synthesized imine polymers, P1, P2, P3, P4, have lower optical band gap values than those of their Schiff bases owing to the extended  $\pi$ -electron conjugation in the polymer backbone. The reduction in the band gap after polymerization made the electronic transition easier and made the polymer more electro-conductive. The highest values of  $\lambda_{\text{onset}}$  and  $E_g$  between the Schiff base and its corresponding polymer were calculated for P2, presumably resulting in an increase in  $\pi$ -conjugation, supported by presence of dihydroxy side group which increased the electron delocalization through the polymer backbone.

The overall absorption of P2 and P4 tailed off to about 700 nm, in comparison to that of P1 and P3, respectively, which resulted in an increase in the conjugated backbones of the polymers.

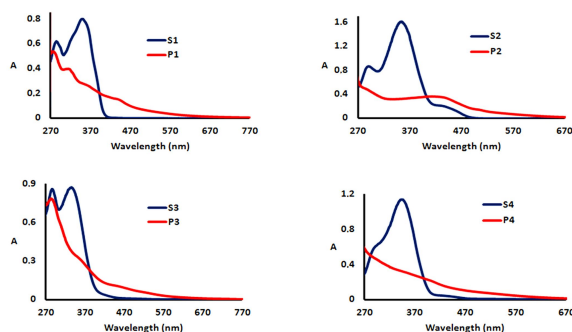


Fig. 9. UV-Vis spectra of (a) S1-P1, (b) S2-P3, (c) S3-P3, and (d) S4-P4.

Cyclic voltammograms CVs of the synthesized compounds were recorded to study their electronic structure and electrochemical properties. The HOMO-LUMO energy levels and electrochemical band gaps  $E'_g$  were calculated using the oxidation  $E_{\text{ox}}$  and reduction peak  $E_{\text{red}}$  potentials. The results were obtained by using the following equations [22]:

$$E_{\text{HOMO}} = -(4.39 + E_{\text{ox}}) \quad (1)$$

$$E_{\text{LUMO}} = -(4.39 + E_{\text{red}}) \quad (2)$$

$$E'_g = E_{\text{LUMO}} - E_{\text{HOMO}} \quad (3)$$

An irreversible peak at both oxidation and reduction areas was observed for the imine polymers. The reduction peak potentials of ( $-\text{HC}=\text{N}$ ) via protonation of imine nitrogen were observed in the range of  $-1.10$  V to  $-1.60$  V for the compounds. The peaks around 1.41 V were caused by the oxidation of phenolic hydroxyl groups to form phenoxy polaron structure ( $\text{PhO}^\bullet$ ) [23].

Table 3 elucidates the inclination of the HOMO elevation and LUMO reduction as a result of polymer formation. Higher  $\pi$ -electron delocalization

Table 2. Thermal analyses results of the synthesized Schiff bases and their imine polymers.

Compounds	TGA					DTA	DSC
	<sup>a</sup> T <sub>on</sub>	<sup>b</sup> T <sub>max</sub>	<sup>c</sup> T <sub>20</sub>	<sup>d</sup> T <sub>50</sub>	% char at 1000 °C	Exo/Endo [°C]	T <sub>g</sub> [°C]/ΔC <sub>p</sub> [J/g·°C]
S1	218	251	246	350	32	–/–	–
P1	170	240, 344, 870	305	771	32	–/–	109/0.553
S2	181	194, 314, 590	238	630	40	–/196	–
P2	219	294, 837	327	792	38.50	–/–	130 / 0.514
S3	261	286	308	865	48	–/285	–/–
P3	271	340, 852	386	899	23.52	–/–	139/1.825
S4	196	204	255	876	45	–/205	–
P4	188	216, 293, 910	481	–	52.45	–/–	134/1.909

<sup>a</sup>The degradation onset temperature [°C]. <sup>b</sup>The maximum weight loss temperature [°C]. <sup>c</sup>Temperature corresponding to 20 % weight loss [°C]. <sup>d</sup>Temperature corresponding to 50 % weight loss [°C]. TGA: thermogravimetric analysis. DTA: differential thermal analysis, DSC: differential scanning calorimetry, T<sub>g</sub>: glass transition temperature, ΔC<sub>p</sub>: change in heat capacity.

Table 3. Electronic structure parameters of the synthesized compounds.

Compounds	<sup>a</sup> HOMO [eV]	<sup>b</sup> LUMO [eV]	<sup>c</sup> E' <sub>g</sub> [eV]	<sup>d</sup> E <sub>g</sub> [eV]	<sup>e</sup> λ <sub>onset</sub> [nm]
S1	–5.74	–2.51	3.23	2.92	440
P1	–5.68	–3.32	2.36	2.39	518
S2	–5.42	–2.78	2.64	2.41	514
P2	–5.53	–2.94	2.59	2.22	557
S3	–5.43	–2.81	2.44	2.97	417
P3	–5.40	–3.36	2.36	2.48	500
S4	–5.52	–3.04	2.40	3.00	414
P4	–5.51	–3.36	2.13	2.79	445

<sup>a</sup>Highest occupied molecular orbital. <sup>b</sup>Lowest unoccupied molecular orbital. <sup>c</sup>Electrochemical band gap. <sup>d</sup>Optical band gap. <sup>e</sup>Absorbance wavelength.

results in receiving an electron easier during reduction process [24]. The presence of electron donating group –OCH<sub>3</sub> group in P1 and P3 facilitates the delocalization of electrons along the polymer chain, leading to lowering E<sub>LUMO</sub>. The values of E'<sub>g</sub>, were in good accordance with E<sub>g</sub> values. The lowest energy gap was calculated for P4 due to more efficient electron delocalization through the polymer chain. Combined effects of the conjugation extent of the polymer chain and the electronic nature of the substituents had a great effect on the energy gap.

### 3.4. Fluorescence characteristics

The photoluminescence (PL) properties of the azomethines studied in DMSO were tabulated

in Table 4. Maximum emission wavelength λ<sub>max</sub> of S1, S2, S3 and S4 in DMSO was observed between 420 nm and 440 nm as excited at 390 nm, 380 nm, 475 nm, 375 nm, respectively. λ<sub>max</sub> of P1, P2, P3 and P4 appeared at 545 nm, 553 nm, 540 nm and 456 nm, when excited at 460 nm, 490 nm, 480 nm and 376 nm, respectively.

As depicted in Fig. 10a and Fig. 10b, when excited at 460 nm and 490 nm, both P1 and P2 emitted green fluorescence light with an emission intensity of 525 and 553, respectively. The monomer S3 revealed a green fluorescence light property as compared to other monomers. As seen Fig. 10c and Fig. 10d, DMSO solutions of S3 and P3 emitted green light at 537 nm and 540 nm under excitation

with 475 nm and 480 nm, respectively. Among the synthesized polymers, only P4 displayed bicolor emission behavior when excited at different wavelengths, whereas the others displayed green-light emission. The emission colors of P4 could be tuned from blue to green upon irradiation of 376 nm and 475 nm, respectively (Fig. 10e). Based on the foregoing results, P4 can be used as a material in light-emitting diodes due to its bicolor (blue and green) light-emitting property.

### 3.5. Electrical properties

Solid state electrical conductivities measurements of P1, P2, P3 and P4 were carried out at the doping times of 0 h, 1 h, 5 h, 24 h, 48 h, 72 h, 96 h and 120 h. The virgin electrical conductivities of P1, P2, P3 and P4 were observed to be  $1.09 \times 10^{-9}$ ,  $3.73 \times 10^{-9}$ ,  $8.40 \times 10^{-11}$  and  $2.58 \times 10^{-9}$  S·cm<sup>-1</sup>, respectively. Upon doping with iodine at room temperature in a vacuum desiccator, the conductivity values increased to  $2.51 \times 10^{-7}$  S·cm<sup>-1</sup>,  $4.0 \times 10^{-7}$  S·cm<sup>-1</sup>,  $3.33 \times 10^{-7}$  S·cm<sup>-1</sup> and  $5.57 \times 10^{-7}$  S·cm<sup>-1</sup>, for P1, P2, P3 and P4, respectively, owing to the conjugation in polymer structures. Electronegative nitrogen atom of (–CH=N) group was able to coordinate with iodine [25]. The results revealed that the electrical conductivities of iodine-doped pellets of all synthesized polymers were increased by about two orders of magnitude in 120 hours. When the polymers were doped with iodine, the conductivity of the polyimines increased remarkably with the increase in doping time at room temperature, but then stabilized. It shows that the polymers were fully saturated with iodine vapor to obtain optimum conductivity. Unlike this, the conductivity of P3 increased by about four orders of magnitude and reached to  $3.33 \times 10^{-7}$  S·cm<sup>-1</sup>. The highest electrical conductivity of  $5.57 \times 10^{-7}$  S·cm<sup>-1</sup> was obtained for P4, which is coherent with CV result.

Opposite relation between  $E'_g$  and the conductivity values indicated that the lowest  $E'_g$  value of P4 resulted in the highest conductivity value as well. Consequently, it can be concluded that the polymers are semi-conducting structures.

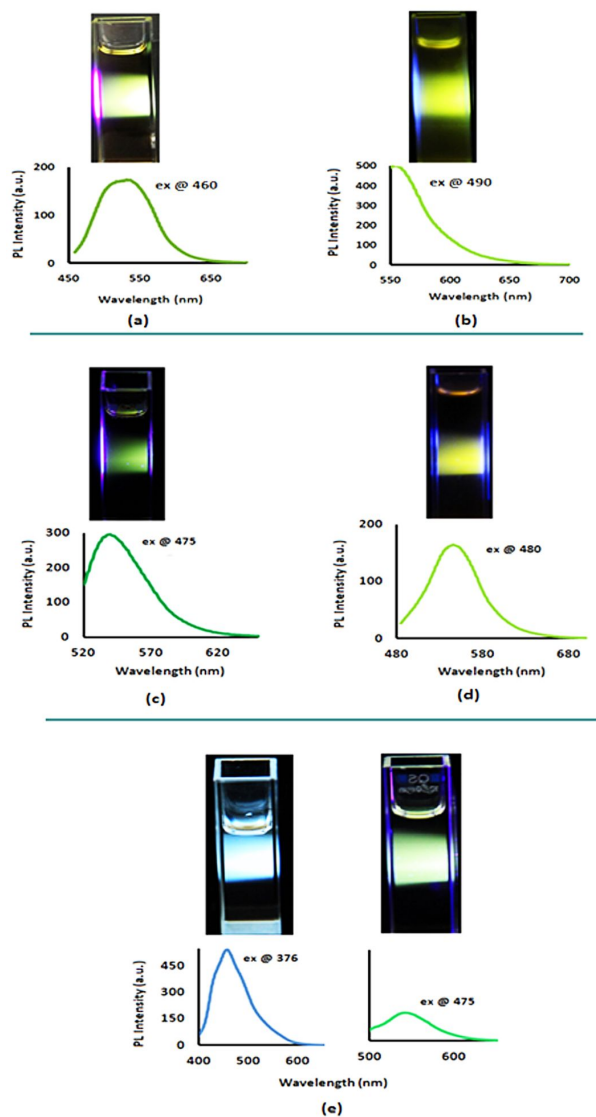


Fig. 10. Photographs of (a) P1, (b) P2, (c) S3, (d) P3, and (e) P4 solutions, and the corresponding PL spectra of P1, P2, S3, P3 and P4 in DMSO.

### 3.6. Morphological properties

The morphological features of the synthesized phenoxy-imine polymers P1, P2, P3, and P4 were obtained by field emission scanning electron microscopy (FE-SEM) technique. Fig. 11 shows FE-SEM images of imine polymers in powder form at different magnifications. As seen in FE-SEM images, the polymer surface is smooth without any specific holes or cracks within the regular FE-SEM resolution. From P1 to P3,

Table 4. PL spectral data of the synthesized compounds in DMSO.

Compound	<sup>a</sup> $\lambda_{\text{ex}}$	<sup>b</sup> $\lambda_{\text{max(Em)}}$	<sup>c</sup> $I_{\text{Em}}$
S1	390	420	20
P1	460	545	176
S2	380	440	125
P2	490	553	497
S3	475	500	297
P3	480	540	134
S4	375	440	220
P4	376	456	542

<sup>a</sup>Excitation wavelength for emission. <sup>b</sup>Emission wavelength for excitation. <sup>c</sup>Maximum emission intensity.

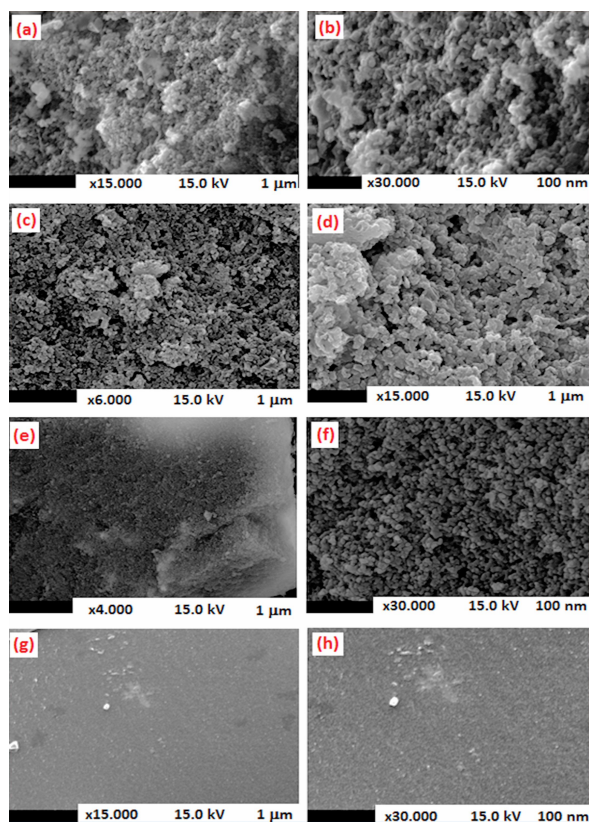


Fig. 11. FE-SEM images of imine polymers P1 (a), (b); P2 (c), (d); P3 (e), (f); P4 (g), (h).

the morphology of the polymers takes a form of smoother and more homogeneous spherical granular structures due to the presence of polyphenol particles (Fig. 11a to Fig. 11d). P4 shows a quite smooth and uniform morphology due to longer  $\pi$ -conjugated backbone (Fig. 11e to Fig. 11f).

## 4. Conclusions

A simple and effective synthesis of green light emitter of polyimines can be developed via OP taking place through C–C (phenylene) and C–O–C (oxyphenylene) type couplings. A series of  $\pi$ -conjugated aromatic polyimines containing hydroxyl groups (phenoxy-imine polymers) have been prepared and their molecular structures were characterized by FT-IR and NMR analyses. We have used UV-Vis and CV techniques to study the electronic structures of  $\pi$ -conjugated aromatic phenoxy-imine polymers with the purpose of shedding light on the effects of molecular structure. The results confirmed the potential of this class of polymers as electroactive and photoactive materials. This study described the optical and thermal properties of the synthesized polymers which revealed that the synthesized polyphenols with imine moieties and high molecular weight were thermostable. In terms of implementation, the azomethine-based compounds could improve the photophysical, thermal and morphological properties of P4. Fluorescent spectral studies indicated that two different emission colors of blue and green were achieved by exciting P4 with UV (376 nm) and blue light (476 nm), presenting P4 as a good candidate for both blue and green-light emitter material with useful thermal stability and smooth homogeneous surface. The results clearly showed that the structure and activity relationship could be used to estimate the morphological and electro-optical properties of conjugated polymers.

Polyphenols with imine moieties along the polymer backbone revealed increased thermal stability and conductivity in photovoltaic areas. P4 had the largest  $\pi$ -conjugation, which was coincident with its highest conductivity. It makes them suitable to be used as semiconducting materials in electronic, optoelectronic and photovoltaic applications.

## References

- [1] BREDAS J.L., CHANCE R.R., *Conjugated polymeric materials: opportunities in electronics, optoelectronics and molecular electronics*, Springer, 1990.
- [2] MCNEILL C.R., GREENHAM N.C., *Adv. Mater.*, 21 (2009), 3840.
- [3] HIDE F., DIAZ-GARCIA M.A., SCHWARTZ B.J., HEEGER A.J., *Accounts Chem. Res.*, 30 (1997), 430.
- [4] ADAMS R., BULLOCK R., WILSON W.C., *J. Am. Chem. Soc.*, 45 (1923), 521.
- [5] NIU H.J., HUANG Y.D., BAI X.D., LI X., *Mater. Lett.*, 58 (2004), 2979.
- [6] KATON J.E., *Organic Semiconducting Polymers*, Marcel Dekker, New York, 1970.
- [7] CERRADA P., ORIO L., PINOL M., SERRANO J.L., ALONSO P.J., PUERTOLAS J.A., IRIBARREN I., GUERRA S.M., *Macromol.*, 32 (1999), 3565.
- [8] OGIRI S., IKEDA M., KANAZAWA A., SHIONO T., IKEDA T., *Polymer*, 40 (1999), 2145.
- [9] MAMEDOV B.A., VIDADI Y.A., ALIEVA D.N., *Polym. Int.*, 43 (1997), 126.
- [10] KAYA I., VILAYETOGLU A.R., TOPAK H., *J. Appl. Polym. Sci.*, 85 (2002), 2004.
- [11] MART H., *Des. Monomers Polym.*, 9 (2006), 551.
- [12] SIMIONESCU C.I., GRIGORAS M., CIANGA I., DIACONU I., FARCAS A., *Polym. Bull.*, 32 (1994), 257.
- [13] SIMIONESCU C.I., IVANIOIU M., CIANGA I., GRIGORAS M., DUCA A., COCARLA I., *Angew. Macromol. Chem.*, 239 (1996), 1.
- [14] NG S.C., CHA H.S.O., WONG P.M.L., TAN K.L., TAN B.T.G., *Polymer*, 39 (1998), 4963.
- [15] KAYA I., ÇULHAOĞLU S., ŞENOL D., *Chem. Pap.*, 61 (2007), 199.
- [16] KAYA I., BILICI A., *J. Appl. Polym. Sci.*, 104 (2007), 3417.
- [17] RYU K., MCELTON J.P., POKORA A.R., CYRUS W., DORDICK J.S., *Biotechnol. Bioeng.*, 42 (1993), 807.
- [18] YILDIRIM M., KAYA I., *Synth. Met.*, 162 (2012), 436.
- [19] SOLMAZ R., KARDAS G., *Prog. Org. Coat.*, 64 (2009), 81.
- [20] BILGE S., KILIC Z., HAYVALI Z., HOKELEK T., SAFRAN S., *J. Chem. Sci.*, 121 (2009), 989.
- [21] COLLADET K., NICOLAS M., GORIS I., LUTSEN I., VANDERZANDE D., *Thin Solid Films*, 451 (2004), 7.
- [22] CERVINI R., LI X.C., SPENCER G.W.C., HOLMES A.B., MORATTI S.C., FRIEND R.H., *Synth. Met.*, 84 (1997), 359.
- [23] BILICI A., KAYA I., YILDIRIM M., DOGAN F., *J. Mol. Catal. B: Enzym.*, 64 (2010), 89.
- [24] CHEN J.C., *Polymer*, 52 (2011), 954.
- [25] GRIGORAS M., CATANESCU C.O., *J. Macromol. Sci. C*, 44 (2004), 131.

Received 2017-03-20  
Accepted 2018-05-04